International Research Journal of Engineering and Technology (IRJET) e-ISSN: 2395-0056
Volume: 08 Issue: 01 | Jan 2021 www.irjet.net p-ISSN: 2395-0072

Performance Analysis of Control Strategies in Wind- Diesel System

Hitesh Joshi[1], A. K. Swami[2]

[1]Ph.D. Scholar, Department of Electrical Engineering, G.B.P.U.A&T, Pantnagar, Uttarakhand
[2]Professor, Department of Electrical Engineering, G.B.P.U.A&T, Pantnagar, Uttarakhand

---

Abstract - *This paper presents the performance analysis of various control strategies developed for the wind energy conversion system (WECS) with permanent magnet synchronous generator (PMSG) and a diesel engine driven generator (DG) set of a standalone hybrid system with a battery energy storage system (BESS). At the point of common coupling (PCC) the voltage is controlled using the synchronous reference frame (SRF) and enhanced phase locked loop (EPLL) theory for the switching of voltage source converter (VSC) of BESS and the maximum power point tracking (MPPT) is achieved for WECS with a perturb and observe (P&O) technique for the switching of a dc-dc boost converter. Simulation results of developed model of proposed standalone hybrid system, which is developed in MATLAB demonstrate performance of both the controllers and power quality improvement of the hybrid system.*

Key Words: WECS, PMSG, DG, BESS, SRF, DSOGI, EPLL, P&O.

1. INTRODUCTION

Throughout the long term, in spite of the best endeavours of industry architects and electric utilities, there have been a considerable level of distantly found consumers living without electricity even to illuminate their lamps. The public authority organizations and public utilities are confronting on several issues because of which the circumstance isn't improving. Quite possibly the main imperatives being the locally accessible expensive fuel assets utilized in supplying of power. To challenge this problem, the harnessing of wind energy for low cost electric power generation could be a prominent and quite promising option, as such, the power from the wind is accessible plentifully all over the earth's surface and also the fast advancement of innovation in this field has inspired to generate large amount of energy from wind to deliver electrical power feasibly in these remote regions.

The standalone systems along with the battery storage are used when there is excess power generation as well as these systems provide balancing of loads during low generation or peak load demand. Therefore, BESSS design and size calculation are important for isolated loading conditions as reported in [1-2]. Microgrid applications incorporating optimum charging and reliable operation with battery charging control is also reported in [3-4]. Hybrid combinations of wind energy conversion system and DG set are one of such, where the wind power is stored in battery and the excess power is utilized to supply the load, while DG set provides AC power to the load [5-6]. This configuration helps to reduce the fuel consumption and economically utilizes the conventional energy resources.

In this paper diesel engine with synchronous generator is reported, which is better due to magnet-less rotor, no cogging torque, no rotor copper losses and lower noise than other brushless generators [7-8]. DG is connected to the PMSG based WECS through VSC with BESS at DC bus. Performance of the VSC as a controller depends on the method for extracting the reference signals to compensate harmonics, regulate the PCC voltage and reactive power requirement of the load [9]. Already several indirect control techniques have been designed for the controller like Power balance theory, PQ theory, SRF theory etc. to estimate reference supply current through computation of positive sequence fundamental current component of load current [10-11]. Here comparison of two control techniques viz. SRF and EPLL is used in controller to meet out all necessary requirement of control. WECS generated AC power is converted into DC power using diode bridge rectifier, followed by DC-DC boost converter than fed to the BESS. BESS provides load leveling during load fluctuations and wind variations. Gate pulse for boost converter is given through MPPT using P&O method [12]. Fig – 1 shows the diagram of the proposed wind-diesel hybrid system.

2. MODELING OF WIND ENERGY GENERATION SYSTEM

2.1 Modeling the Wind Turbine System

The actual modeling of the wind turbine based on the aerodynamic non-linear power characteristics is denoted as P_m

And is basically written in the equation form [13,14] as:

$$P_m = 0.5\rho A v^3 C_p(\lambda, \beta) \quad (1)$$

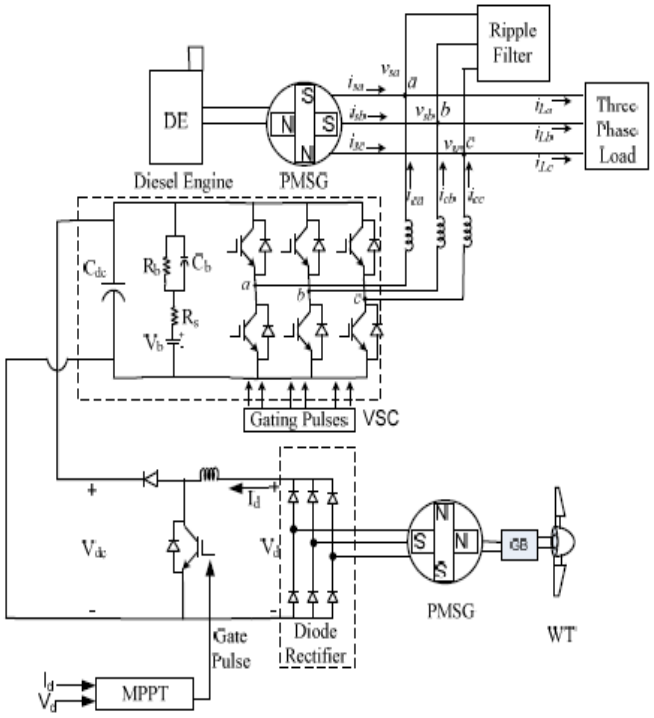

Fig – 1: A diagram of wind-diesel hybrid system

where A, represents the swept area (in metres) of rotor of the turbine blades and, ρ is defined as the density of air (in kg/m^2), v is the wind velocity (in m/sec), C_p denotes the coefficient of performance, β denotes the angular position of the pitch of the blades and λ is described with a ratio between the tip of the rotor blade divided by the velocity of the wind, which is typically represented as the tip speed ratio (λ) of the turbine, as such given by:

$$\lambda = \frac{\omega_m * R}{v} \quad (2)$$

The coefficient of performance of the wind turbine blades reflects the relationship among the tip-speed ratio, λ [15] and the power coefficient, C_p of the wind turbine system and is depicted in Fig.2.The mathematical relation involving C_p is given by:

$$Cp\ (\lambda, \beta) = [0.22\left(\frac{116}{\lambda i} - 0.4\beta - 5\right)\exp(\frac{-12.5}{\lambda i})] \quad (3)$$

where λ_i is given as :

$$\lambda_i = \left[\frac{1}{(\lambda+0.089)} - \frac{0.035}{(\beta^3+1)}\right]^{-1} \quad (4)$$

When the value of the pitch blade is $\beta = 0^o$ then the value of tip speed ratio is simultaneously taken as, $\lambda = 7.511$, then under these conditions C_p has its maximum value which occurs at $C_{pmax} = 0.4526$ (Fig - 2). So this is the value of C_p at which the maximum energy from wind is being captured and through this we can easily get the optimal point of operation of λ_{opt}.

The aerodynamic or mechanical torque T_m(N-m) can therefore be expressed in terms of the ratio of power as captured directly from the wind system P_m(in watts) with the speed of a rotor of wind turbine, denoted as ω_m(rad/s), hence this ratio could be expressed as:

$$T_m = \frac{P_m}{\omega_m} \quad (5)$$

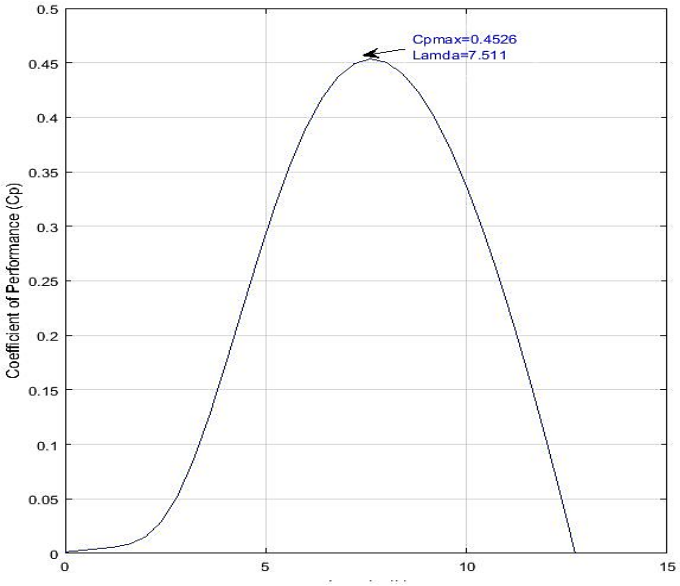

Fig – 2: C_p *vs* λ curve

2.2 Model of Permanent Magnet Synchronous Generator

The model which is mainly used to define the dynamic behaviour of the PMSG in reference d-q frame could then be demonstrated [16-17,18] considering the equations below:

$$V_{ds} = -R_s i_{ds} + \frac{d}{dt}\varphi_{ds} - \omega\varphi_{qs} \quad (6)$$

$$V_{qs} = -R_s i_{qs} + \frac{d}{dt}\varphi_{qs} - \omega\varphi_{ds} \quad (7)$$

The equations involving the flux linkage are described as:

$$\varphi_{ds} = -L_{ds} * i_{ds} + \varphi_f \quad (8)$$

$$\varphi_{qs} = L_{qs} * i_{qs} \quad (9)$$

The equation that derives the synchronous generator mechanically can be evaluated as:

$$J\frac{d}{dt}(\Omega) = T_w - T_e - B*\Omega \quad (10)$$

for the above equation, the electromagnetic torque been represented in d-q reference frame as:

$$T_e = P\ (\varphi_{ds} * i_{qs} - \varphi_{qs} * i_{ds}) \quad (11)$$

in which :

$\Omega = \frac{d}{dt}\theta$, $\omega = \frac{d}{dt}\theta_e = p\Omega$, $\theta_e = p\theta$ (12)

where R_s denotes the resistance in the stator, L_{ds} and L_{qs} are the direct-axis and quadrature-axis inductances in the stator, φ_{ds} and φ_{qs} are the direct-axis and quadrature-axis fluxes, respectively. φ_f is the flux in the field circuit, T_w is the torque available from the wind and been applied to the PMSG rotor shaft, T_e is used to represent the electromagnetically induced torque, p is used to express the no. of poles in pairs, B is the co-efficient of damping, J is the inertia constant (kg/m^2), ω represents the generator angular rotor speed expressed in electrical degrees, Ω is the angular speed in mechanical radians, θ is the position of mechanical rotor, and θ_e is the position of the electrical rotor.

3. CONTROL METHODS

In this system two controllers are used for VSC and MPPT controller of boost converter for variable speed WECS.

Both the two PLL based algorithms used in the paper extract the fundamental components of the load current to evaluate the reference supply currents.

Terminal voltage V_t is calculated using phase voltages as,

$$V_t = \sqrt{2/3}\,(v_{sa}^2 + v_{sb}^2 + v_{sc}^2) \quad (13)$$

where v_{sa}, v_{sb} and v_{sc} are phase voltages.

The in-phase unit templates are expressed as,

$$u_{pa} = \frac{v_{sa}}{V_t}, u_{pb} = \frac{v_{sb}}{V_t}, u_{pc} = \frac{v_{sc}}{V_t} \quad (14)$$

The Quadrature unit templates are estimated as,

$$u_{qa} = \frac{u_{pc} - u_{pb}}{\sqrt{3}} \quad (15)$$

$$u_{qb} = \frac{3u_{pa+}u_{pb-u_{pc}}}{2\sqrt{3}} \quad (16)$$

$$u_{qc} = \frac{-3u_{pa+}u_{pb-u_{pc}}}{2\sqrt{3}} \quad (17)$$

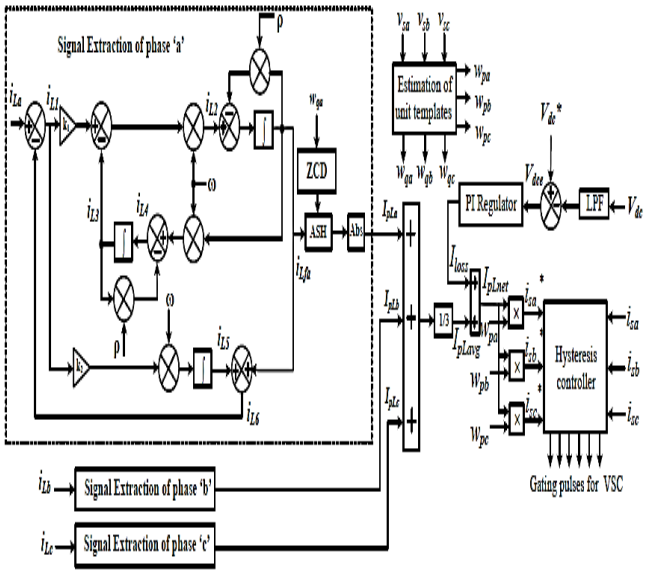

Fig – 3: The control strategy based on PLL

Expressions for active and reactive power component of the 3-φ load currents are as,

$$I_{sp} = \frac{I_{Lpa}+I_{Lpb}+I_{Lpc}}{3} \quad (18)$$

$$I_{sq} = \frac{I_{Lqa}+I_{Lqb}+I_{Lqc}}{3} \quad (19)$$

The fundamental reference active and reactive power components of the 3-φ input currents are calculated as,

$$i_{spa}^* = I_{sp} \times u_{pa}\,, i_{spb}^* = I_{sp} \times u_{pb}\,, i_{spc}^* = I_{sp} \times u_{pc} \quad (20)$$

$$i_{sqa}^* = I_{sq} \times u_{qa}\,, i_{sqb}^* = I_{sq} \times u_{qb}\,, i_{sqc}^* = I_{sq} \times u_{qc} \quad (21)$$

The 3-φ reference input currents are given as,

$$i_{sa}^* = i_{spa}^* + i_{sqa}^*\,, i_{sb}^* = i_{spb}^* + i_{sqb}^*\,, i_{sc}^* = i_{spc}^* + i_{sqc}^* \quad (22)$$

3-φ reference input currents ($i_{sa}^*, i_{sb}^*, i_{sc}^*$) and measured input currents (i_{sa}, i_{sb}, i_{sc}) are compared to generate current error signal u(t) for every phase. VSC is switched using hysteresis control as,

If u(t) > upper limit of hysteresis band; lower switch on.

If u(t) < lower limit of hysteresis band; upper switch on.

4. MPPT ALGORITHM

Duty cycle is calculated directly according to the MPPT value and used to regulate the output of boost converter to keep the DC link voltage 700V. The flowchart for P&O method is shown in fig 3. Duty cycle is reduced if the functional point is towards left hand side and it is increased for right hand side of Maximum power point. With the variation in duty cycle the boost converter keeps the output voltage constant across the DC bus.

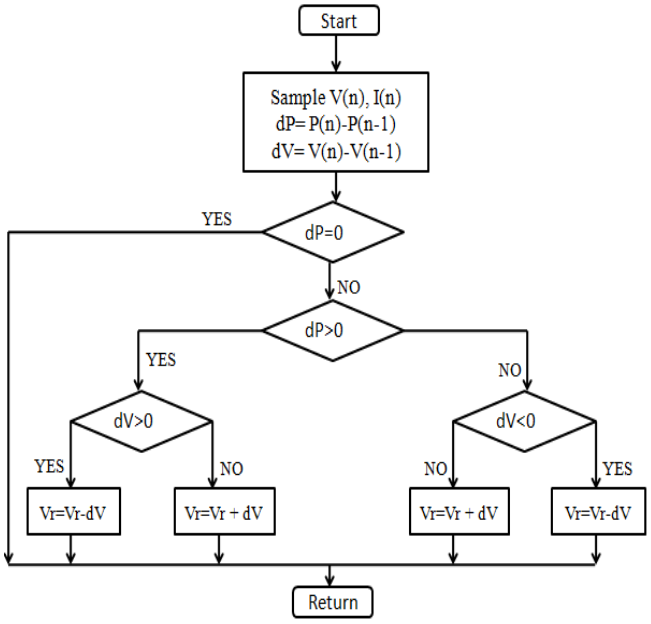

Fig – 4: Flowchart of P&O MPPT

5. Selection of BESS and Boost Converter

The selection of battery system voltage depends on synchronous generator line to line voltage of the DG. The DC bus voltage is computed as,

$$V_{dc} = \frac{2\sqrt{2}}{\sqrt{3}} V_L \quad (23)$$

The V_{dc} from this equation is obtained as 700 V. Therefore, the battery bank is selected 760V. Thevenin's model is used to describe BESS, where (C_b) capacitance and resistance (R_b) connected parallel along with series connected internal resistance (R_s) and an ideal voltage source of voltage 700 V. Equivalent capacitance C_b is calculated as [19] as,

$$C_b = \frac{(kW.h*3600*1000)}{0.5(V_{oc\,max}^2 - V_{oc\,min}^2)} \quad (24)$$

where V_{ocmin} and V_{ocmax} are the open circuit voltages with minimum and maximum values under fully discharged and fully charged states of battery system.

The output voltage of boost converter is calculated as,

$$V_{dc} = \frac{V}{(1-D)} \quad (25)$$

To limit the peak to peak current ripple (ΔI_L) an inductor (L) with given switching frequency is calculated as,

$$L = \frac{V_{DC}}{(4 \times f_s \times \Delta I_L)} \quad (26)$$

6. SIMULATION RESULTS

In Fig.7, the performance of MPPT controller under increase in wind speed from 8 m/s to 12 m/s at 2.5 kW, 3-phase linear load is depicted. Till 0.2s, the wind speed is 8 m/s and there is a rated power generation through PMSG. At 0.2s, there is an increment in wind speed and also in WECS power generation. WECS PMSG shaft speed increases with increase in wind speed to achieve MPPT. It is noticed that wind power is increased as the wind speed accelerates to 12 m/s. Regulated PCC voltage and sinusoidal supply current at DG terminals (vsa and isa) justify satisfactory working of VFC.

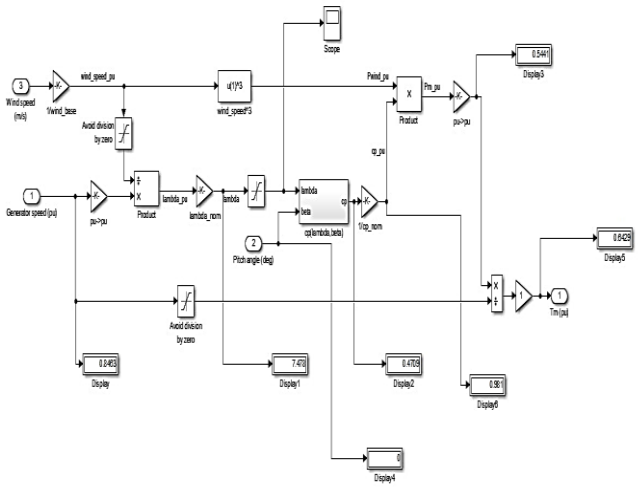

Fig – 5: Simulation model of wind system

At 0.2s, increase in wind speed is 12 m/s therefore WECS power generation also increases according to maximum power capture scheme of boost converter using P&O and terminal voltage, supply voltage and supply currents are made balanced and constant by VFC.

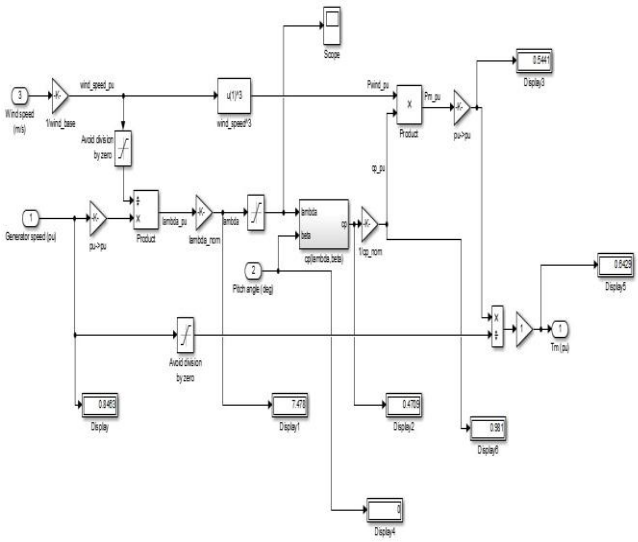

Fig – 6: Simulation model of P&O MPPT

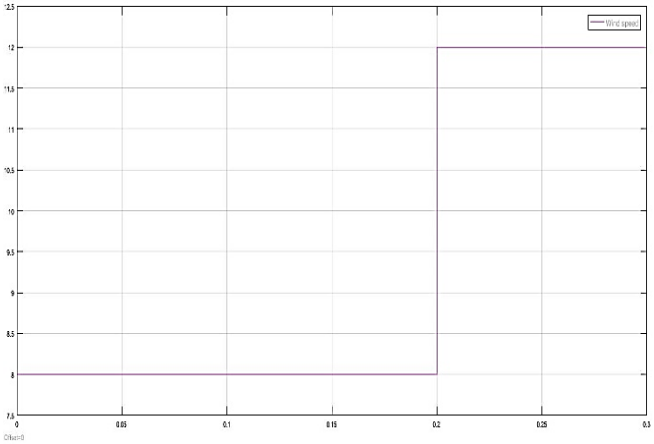

Fig – 7: Wind speed variation

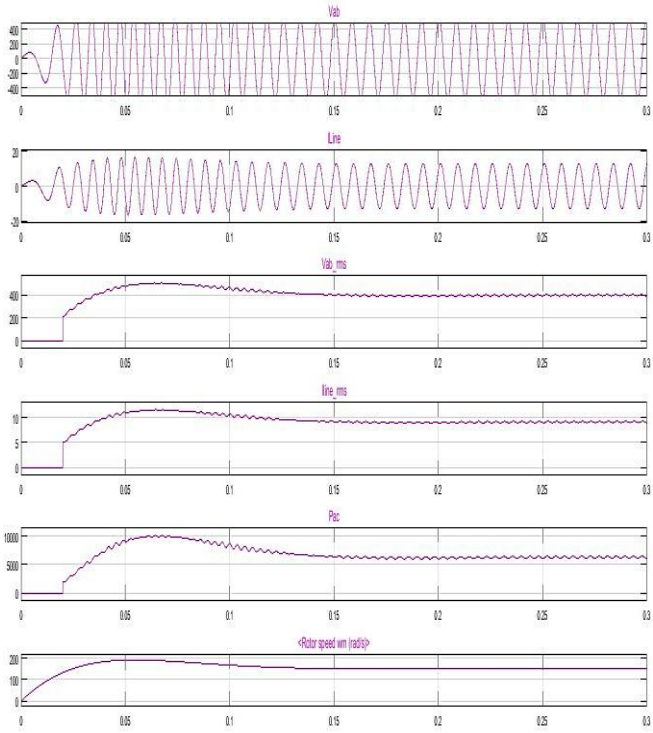

Fig – 8: Line voltage, line current, rms voltage and current, power and rotor speed

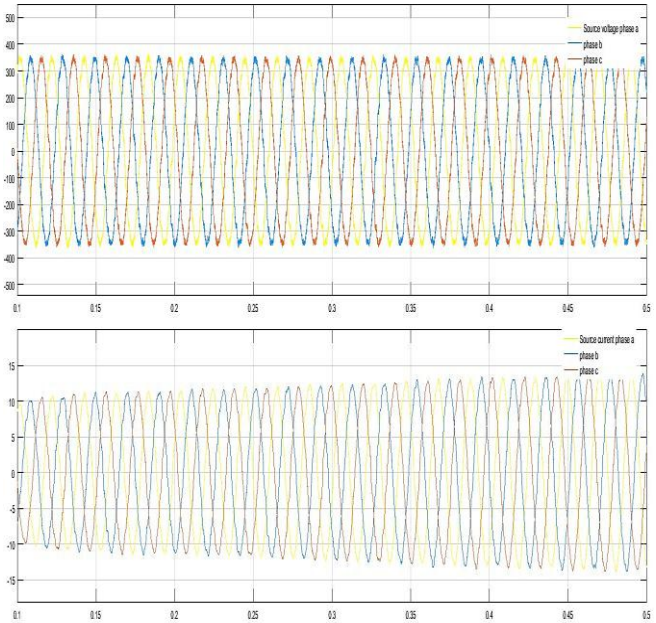

Fig – 9: Source voltage and current of Diesel generator

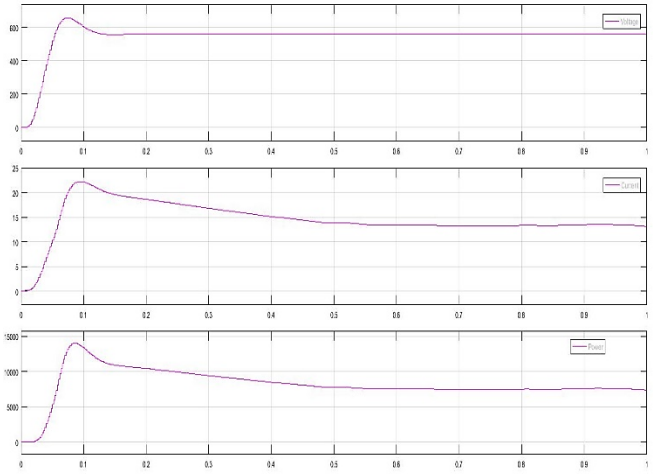

Fig – 10: MPPT voltage, current and power

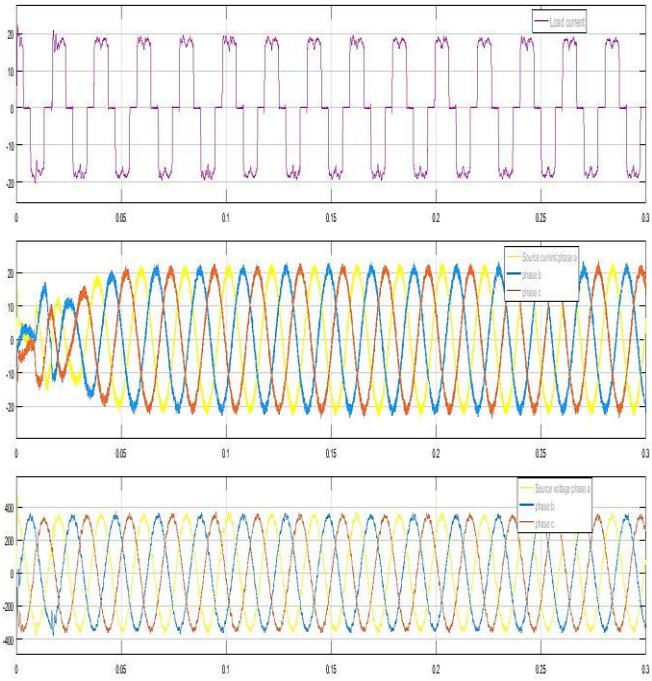

Fig – 11: Load current, source current and source voltage using SRF theory

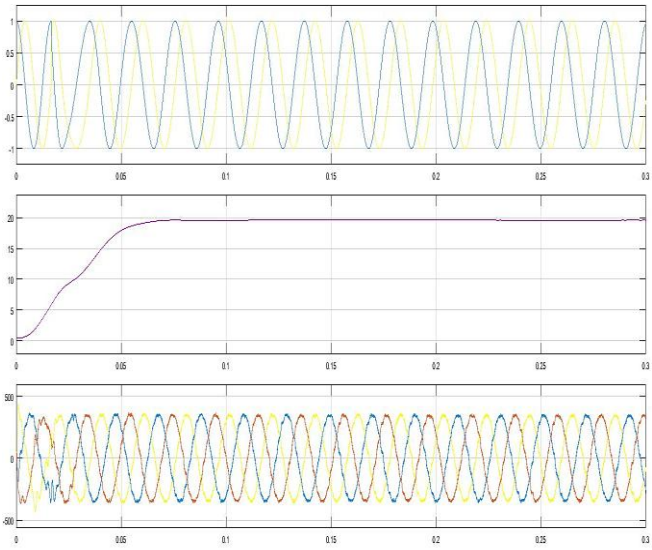

Fig – 12: Sine-Cos waveform generation

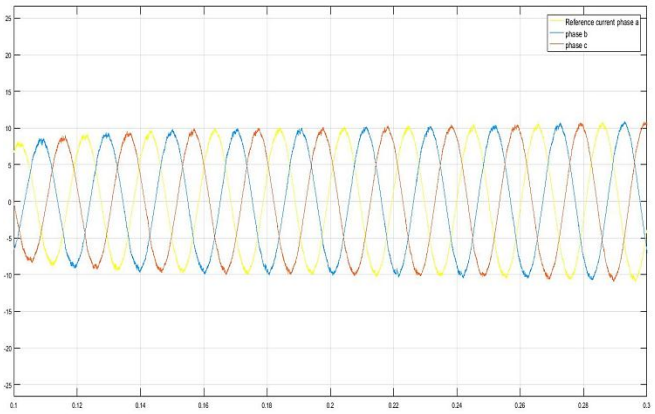

Fig – 13: Reference current generated by controller

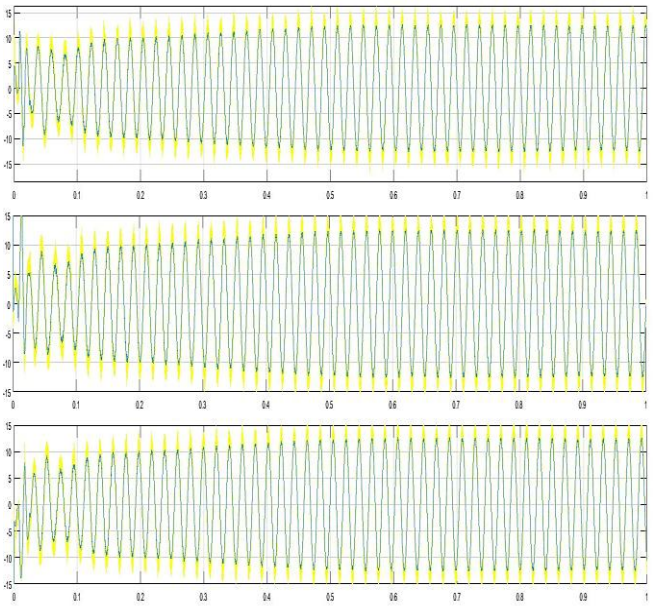

Fig – 14: Phase matching of the source and reference currents

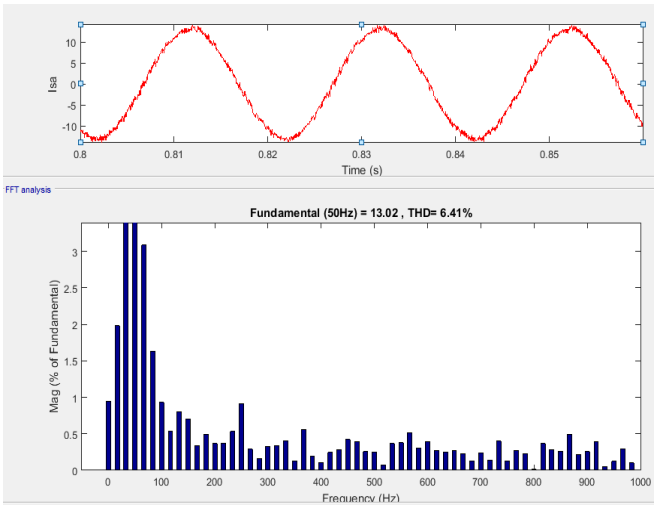

Fig – 15: FFT analysis of source current with SRF technique

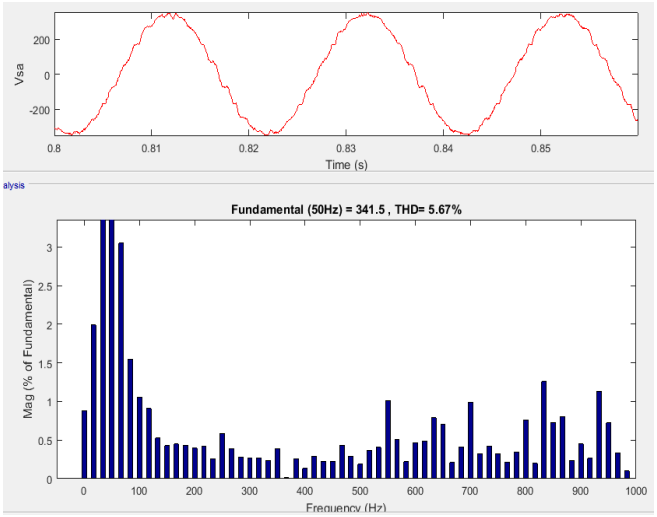

Fig – 16: FFT analysis of source voltage with SRF technique

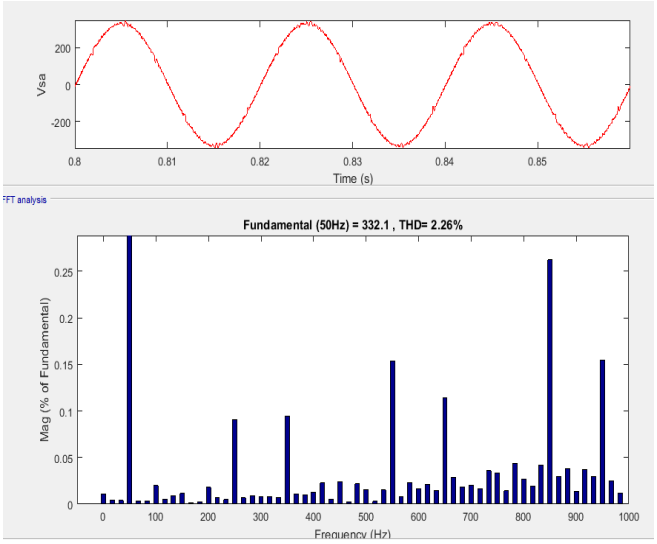

Fig – 17: FFT analysis of source voltage with EPLL technique

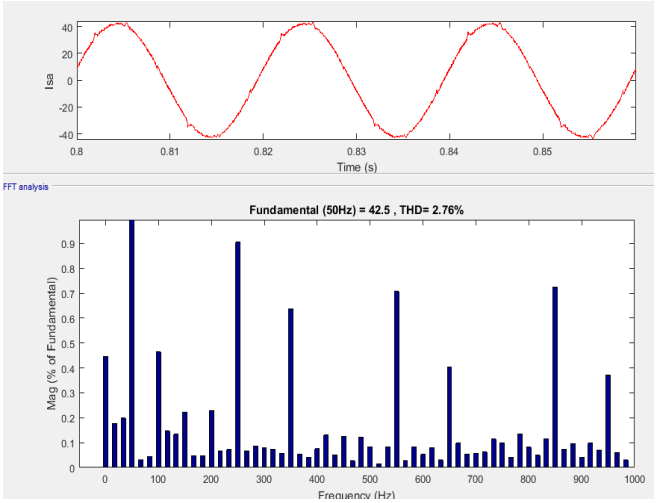

Fig – 18: FFT analysis of source current with EPLL technique

The total harmonic distortion (THD) of source voltage and current is less than 3% (fig – 17, 18) with the EPLL technique whereas the THD with SRF technique is greater than 5% (fig – 15, 16).

7. CONCLUSION

An isolated wind-diesel hybrid system has been implemented in MATLAB Simulink. A mechanical sensor less approach has been used for achieving MPPT through perturb and observe technique. The PMSG configuration provided for the wind energy system is simple and robust and the ac power is converted to the dc using the boost converter. VFC provided the load balancing, reactive power compensation, and harmonics elimination and voltage regulation at PCC under nonlinear loads operation using both SRF and EPLL techniques. The comparative analysis shows that the EPLL technique is better in compensating the harmonics as compared to the SRF method.

8. REFERENCES

1. Arabali, M. Ghofrani, M. Etezadi-Amoli, M.S. Fadali, “Stochastic Performance Assessment and Sizing for a Hybrid Power System of Solar/Wind/Energy Storage,” IEEE Transactions on Sustainable Energy, vol.5, no.2, pp.363-371, April 2014.
2. B. Singh, and S. Sharma, “Design and Implementation of Four-Leg Voltage-Source-Converter-Based VFC for Autonomous Wind Energy Conversion System,” IEEE Transactions on Industrial Electronics, vol.59, no.12, pp.4694-4703, Dec. 2012.
3. Hongyu Zhu, Donglai Zhang, H.S. Athab, Bin Wu, and Yu Gu, “PV Isolated Three-Port Converter and Energy-Balancing Control Method for PV-Battery Power Supply Applications,” IEEE Transactions on Industrial Electronics, vol.62, no.6, pp.3595-3606, June 2015.
4. M. Hosseinzadeh, and F.R. Salmasi, “Power management of an isolated hybrid AC/DC micro-grid with fuzzy control of battery banks,” IET on Renewable Power Generation, vol.9, no.5, pp.484-493, 2015.
5. B. Singh, R. Niwas, and S. Dube, “Load Leveling and Voltage Control of Permanent Magnet Synchronous Generator Based DG Set for Standalone Supply System,” IEEE Transactions on Industrial Informatics, vol.10, no.4, pp.2034-2043, Nov. 2014.
6. S. Singla, Y. Ghiassi-Farrokhfal, and S. Keshav, “Using Storage to Minimize Carbon Footprint of Diesel Generators for Unreliable Grids,” IEEE Transactions on Sustainable Energy, vol.5, no.4, pp.1270-1277, Oct. 2014.
7. Poopak Roshanfekr, Sonja Lundmark, Torbjorn Thiringer, and Mikael Alatalo, “A synchronous reluctance generator for a wind application

compared with an interior mounted permanent magnet synchronous generator," in Proc. of 7th IET International Conference on Power Electronics, Machines and Drives (PEMD), 2014, , pp.1,5, 8-10 April 2014.

8. Y.H.A Rahim, J.E. Fletcher, and N.E.A. Hassanain, "Performance analysis of salient-pole self-excited reluctance generators using a simplified model," IET on Renewable Power Generation, vol.4, no.3, pp.253, 260, May 2010.
9. B. Singh, and J. Solanki, "Load Compensation for Diesel Generator- Based Isolated Generation System Employing DSTATCOM," IEEE Trans. on Industry Applications, vol.47, no.1, pp.238,244, Jan.-Feb. 2011.
10. B. Singh, D.T. Shahani, and A K. Verma, "IRPT based control of a 50 kw grid interfaced solar photovoltaic power generating system with power quality improvement," in Proc. of 4th IEEE International Symposium on Power Electronics for Distributed Generation Systems (PEDG), 2013, pp.1,8, 8-11 July 2013.
11. G. Bhuvaneswari, and M.G. Nair, "Design, Simulation, and Analog Circuit Implementation of a Three-Phase Shunt Active Filter Using the I cosΦ Algorithm," IEEE Trans. on Power Delivery, vol.23, no.2, pp.1222,1235, April 2008.
12. A.M. Eltamaly, 'Modeling of Wind Turbine Driving Permanent Magnet Generator with Maximum Power Point Tracking System', J. King Saud Univ., Vol. 19, Eng. Sci. (2), pp. 223- 237, Riyadh (1427H./2007).
13. J. S. Thongam, P. Bouchard, H. Ezzaidi and M. Ouhrouche, "Wind Speed Sensorless Maximum Power Point Traking Control of Variable Speed Wind Energy Conversion System", Electric Machines and Drives Conference, pp. 1832-1837, 2009.
14. J. Villar Alé, F. Daher Adegas and G. Cirlo da Silva Simioni, 'Maximum Power Point Tracker for Small Wind Turbines Including Harmonic Mitigation', Wind Energy Conference & Exhibition European 2006.
15. J. Nandana, P. K. Murthy, and S. Durga, "VSC-HVDC Transmission System Analysis Using Neural Networks," International Journal of Engineering Science and Innovative Technology (IJESIT), vol. 2, May 2013.
16. S. Kazmi, H. Goto, H.-J. Guo, and O. Ichinokura, "A novel algorithm for fast and efficient speed-sensorless maximum power point tracking in wind energy conversion systems," IEEE Transactions on Industrial Electronics, vol. 58, no. 1, pp. 29–36, 2011.
17. D. D. C. Lu and Q. N. Nguyen, "A photovoltaic panel emulator using a buck–boost dc/dc converter and a low cost micro-controller," Solar Energy, vol. 86, no. 5, pp. 1477–1484, May 2012.
18. N. Mohan, T. Undeland, and W. Robbins 'Power Electronics Converters, Application and Design ', New York: John Wiley & Sons, 2003.
19. P.K. Goel, B. Singh, S.S. Murthy, and N. Kishore, "Isolated Wind– Hydro Hybrid System Using Cage Generators and Battery Storage," IEEE Trans. on Industrial Electronics, vol.58, no.4, pp.1141,1153, April 2011.